Achievable Rates of MIMO-ISI Systems with Linear Precoding and Iterative LMMSE Detection

Xiaojun Yuan*, Li Ping*, and Aleksandar Kavcic†
* Department of Electronic Engineering, City University of Hong Kong, Hong Kong
† Department of Electronic Engineering, University of Hawaii at Manoa, Honolulu, HI, USA, 96822

Abstract—**In this paper, we consider the performance analysis of multiple-input multiple-output (MIMO) inter-symbol interference (ISI) systems involving linear-precoding (LP) and iterative linear minimum mean-square error (ILMMSE) detection. The main contribution of this paper is an area theorem to evaluate the achievable rate of the proposed LP-ILMMSE scheme. Based on this area theorem, we further optimize the linear precoder to maximize the achievable rate. Numerical results are provided to verify our analysis.**

I. Introduction

The optimal detection of a coded signal in a complicated transmission environment usually requires excessively high complexity. Iterative detection is a low-cost solution in which the overall receiver is decomposed into two or more local processors [1]. The analysis of iterative detection is intriguing. The density evolution technique [2] shows that carefully designed low-density parity-check (LDPC) codes can achieve near-capacity performance in additive white Gaussian noise (AWGN) channels with iterative decoding algorithms. It has been shown in [3] that the achievable rate of an iterative scheme for an erasure channel can be measured by the area under the so-called EXIT curves [4] and the channel capacity is approachable when the two local processors have matched EXIT curves. This area property is extended in [5] to AWGN channels using the measure of minimum mean-square error (MMSE), which establishes a sufficient condition to approach the capacity of a binary AWGN channel with iterative detection.

In this paper, we study the coded multiple-input multiple-output (MIMO) inter-symbol interference (ISI) systems proposed in [6] involving linear precoding (LP) at the transmitter and iterative linear MMSE detection (ILMMSE) at the receiver. The ILMMSE receiver consists of two local processors, namely, the elementary signal estimator (ESE) handling the channel effect and the decoder (DEC) handling the forward-error-control (FEC) coding effect. We prove that the ESE output can be modeled as observations from an AWGN channel provided that the transmission block length is sufficiently large. This allows us to establish an area theorem for the LP-ILMMSE scheme using the renowned MMSE mutual-information relationship [7]. As an application of the area theorem, we further discuss the optimal LP design to maximize the information rate of the scheme. We show that, unlike the approach in [6] which only optimizes the LP for a fixed FEC code, both the LP and the FEC code needs to be optimized, and the resulting LP-ILMMSE scheme can approach the MIMO water-filling capacity.

It is worth mentioning that the extension of the area property to MIMO-ISI systems was attempted in our previous work [8]. The area theorem in [8] is established based on an unjustified assumption, i.e., both the ESE and DEC outputs can be modeled as observations from an AWGN channel. Unfortunately, this AWGN assumption may be far from true in a practical coded MIMO-ISI system. As a major contribution of this paper, we show that the AWGN assumption can be made asymptotically true for the ESE outputs (as the transmission block length tends to infinity) using the aforementioned LP technique. Moreover, the area theorem established in this paper does not rely on the AWGN assumption for the DEC outputs. These differences distinguish the work in this paper from the one in [8].

II. System Description

A generic discrete complex-valued linear system is modeled by a linear equation as

$$\boldsymbol{u} = \boldsymbol{G}\boldsymbol{v} + \boldsymbol{w} \tag{1}$$

where $\boldsymbol{u}$ is the received signal vector, $\boldsymbol{G}$ the system transfer matrix known at both the transmitter and receiver sides, $\boldsymbol{v}$ the transmit signal vector, and $\boldsymbol{w} \sim \mathcal{CN}(\boldsymbol{0}, \sigma^2\boldsymbol{I})$ a white-noise vector. An AWGN channel is a special case of (1) when $\boldsymbol{G} = \boldsymbol{I}$. More general examples of (1) include MIMO and ISI channels. We next describe a transceiver system involving LP and ILMMSE detection over the channel in (1).

A. Linear Precoding

The LP technique proposed in [6] is briefly described as follows. Let the singular value decomposition (SVD) of $\boldsymbol{G}$ be

$$\boldsymbol{G} = \boldsymbol{U}\boldsymbol{\Delta}\boldsymbol{V}^{\mathrm{H}} \tag{2}$$

where $\boldsymbol{\Delta}$ is a diagonal matrix referred to as the channel spectrum, and both $\boldsymbol{U}$ and $\boldsymbol{V}$ are unitary matrices. Assume that $\boldsymbol{v}$ in (1) is produced by a precoding matrix $\boldsymbol{P}$ as

$$\boldsymbol{v} = \boldsymbol{P}\boldsymbol{x} \tag{3a}$$

where $\boldsymbol{x}$ is a length-J vector generated by an FEC code. Denote by x_i the ith entry of $\boldsymbol{x}$. We assume that each x_i is constrained on a signaling constellation $\mathcal{S}$ with the size denoted by $|\mathcal{S}|$. The precoder $\boldsymbol{P}$ is defined as

$$\boldsymbol{P} = \boldsymbol{V}\boldsymbol{W}\boldsymbol{F} \tag{3b}$$

where $\boldsymbol{V}$ is obtained in (2), the power allocation matrix $\boldsymbol{W}$ is a diagonal matrix with non-negative diagonal elements, and the dispersion matrix $\boldsymbol{F}$ is the normalized DFT matrix with the (i, k)th entry given by

$$F(i, k) = J^{-1/2}\exp(-\mathrm{j}2\pi ik/J). \tag{4}$$

Note that, for constrained signaling, the use of the dispersion matrix $\boldsymbol{F}$ can significantly improve the system performance [16]. The optimization of the power allocation matrix $\boldsymbol{W}$ will be discussed in Section V.

At the receiver side, the received vector $\boldsymbol{u}$ is post-processed by a matrix $\boldsymbol{U}^{\mathrm{H}}$:

$$\boldsymbol{y} = \boldsymbol{U}^{\mathrm{H}}\boldsymbol{u}\,. \tag{5}$$

Combining (1)-(3) and (5), and letting

$$\boldsymbol{\eta} = \boldsymbol{U}^{\mathrm{H}}\boldsymbol{w},\ \boldsymbol{H} = \boldsymbol{DF},\ \text{and}\ \boldsymbol{D} = \boldsymbol{\Delta W}, \tag{6a}$$

we obtain an equivalent channel as

$$\boldsymbol{y} = \boldsymbol{Hx} + \boldsymbol{\eta} \tag{6b}$$

where $\boldsymbol{\eta} \sim \mathcal{CN}(\boldsymbol{0}, \sigma^2\boldsymbol{I})$ (as $\boldsymbol{U}$ is unitary). This equivalent channel is illustrated in the upper half of Fig.1.

B. Iterative Detection

For the channel in (1), the optimal receiver needs to jointly consider the channel and coding effects, which may require excessively high complexity. Iterative detection significantly reduces the complexity by processing the two effects separately.

A typical iterative receiver, as illustrated in the lower half of Fig.1, consists of two concatenated local processors: the elementary signal estimator (ESE) and the decoder (DEC). The ESE estimates $\boldsymbol{x}$ based on the observed $\boldsymbol{y}$ in (6b) and the output of the DEC (as if $\boldsymbol{x}$ is un-coded). The DEC performs decoding based on the ESE output. (The DEC does not see the channel observation directly.) The ESE and DEC are executed iteratively for performance improvement.

The decoding operation of the DEC is standard in the literature. We next focus on the ESE operation.

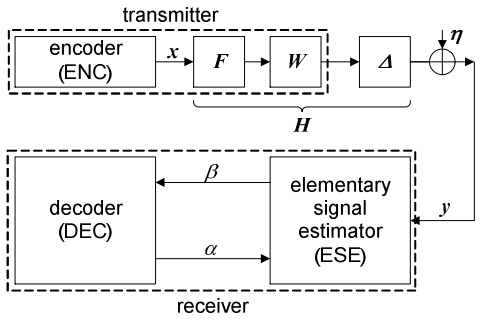

Fig. 1. The transceiver structure of the LP-ILMMSE scheme over the equivalent channel in (6).

C. LMMSE Estimation for the ESE

The ESE follows the LMMSE principle detailed as follows. Denote by α the ESE input (that is also the DEC output). In general, α is a set of J messages as

$$\alpha = \{\alpha_0, \alpha_1, \ldots, \alpha_{J-1}\},$$

and each message α_i is a set of $|\mathcal{S}|$ likelihood values for x_i, i.e.

$$\alpha_i = \{\alpha_i(0), \alpha_i(1), \ldots, \alpha_i(|\mathcal{S}|-1)\},$$

where $\alpha_i(k)$ represents the likelihood of $x_i = s_k \in \mathcal{S}$ prior to the ESE processing, and

$$\sum\nolimits_{k=0}^{|\mathcal{S}|-1} \alpha_i(k) = 1\,.$$

Similar notations are also applicable to the ESE output β.

The *a priori* mean and covariance of $\boldsymbol{x}$ seen by the ESE are denoted by $\boldsymbol{z}$ and $v\boldsymbol{I}$, respectively, where

$$z_i = \sum\nolimits_{k=0}^{|\mathcal{S}|-1} \alpha_i(k) s_k \tag{7a}$$

and

$$v = J^{-1}\sum\nolimits_{i=0}^{J-1}\sum\nolimits_{k=0}^{|\mathcal{S}|-1} \alpha_i(k)\left|s_k - z_i\right|^2\,. \tag{7b}$$

The LMMSE estimator of $\boldsymbol{x}$ given $\boldsymbol{y}$ can be expressed as [9]

$$\hat{\boldsymbol{z}} = \boldsymbol{z} + v\boldsymbol{H}^{\mathrm{H}}\boldsymbol{R}^{-1}(\boldsymbol{y} - \boldsymbol{Hz}) \tag{8a}$$

and the MMSE matrix is given by

$$\boldsymbol{\Omega} = v\boldsymbol{I} - v^2\boldsymbol{H}^{\mathrm{H}}\boldsymbol{R}^{-1}\boldsymbol{H} \tag{8b}$$

where $\boldsymbol{R}$ is the *a priori* covariance matrix of $\boldsymbol{y}$ given as

$$\boldsymbol{R} = v\boldsymbol{H}\boldsymbol{H}^{\mathrm{H}} + \sigma^2\boldsymbol{I}\,. \tag{8c}$$

Following the Turbo principle [1], we calculate the extrinsic mean z_i^{EXT} and variance v_i^{EXT} as (cf., (34) in [8]):

$$(v_i^{\mathrm{EXT}})^{-1} = (\Omega(i,i))^{-1} - v^{-1} \tag{9a}$$

and

$$\frac{z_i^{\mathrm{EXT}}}{v_i^{\mathrm{EXT}}} = \frac{\hat{z}_i}{\Omega(i,i)} - \frac{z_i}{v}\,. \tag{9b}$$

Finally, the outputs of the ESE are calculated as

$$\beta_i(k) = p(x_i = s_k \mid z_i^{\mathrm{EXT}})\,,\ \text{for any } i \text{ and } k. \tag{10}$$

The above ESE operation can be implemented using fast Fourier transform with complexity $O(N\log N)$. More details can be found, e.g., in [6] and [8].

III. Properties of the ESE Output

In this section, we show that the ESE outputs can be treated as observations from an AWGN channel. Let $\rho_i^{\mathrm{EXT}} = 1/v_i^{\mathrm{EXT}}$. We first prove that ρ_i^{EXT} is invariant with respect to the index i.

Lemma 1:

$$\rho_i^{\mathrm{EXT}} = \rho^{\mathrm{EXT}} = \left(\frac{1}{J}\sum_{k=0}^{J-1}\left(\frac{1}{v} + \frac{|D(k,k)|^2}{\sigma^2}\right)^{-1}\right)^{-1} - \frac{1}{v},\ \forall i. \tag{11}$$

Proof: Substituting $\boldsymbol{H} = \boldsymbol{DF}$ and (8c) into (8b), we obtain

$$\boldsymbol{\Omega} = v\boldsymbol{I} - v^2\boldsymbol{F}^{\mathrm{H}}\boldsymbol{D}^{\mathrm{H}}(v\boldsymbol{D}\boldsymbol{D}^{\mathrm{H}} + \sigma^2\boldsymbol{I})^{-1}\boldsymbol{DF}\,.$$

The diagonal entries of $\boldsymbol{\Omega}$ are equal to each other by noting that

$$\begin{aligned}\Omega(i,i) &= v - v^2\boldsymbol{f}_i^{\mathrm{H}}\boldsymbol{D}^{\mathrm{H}}(v\boldsymbol{D}\boldsymbol{D}^{\mathrm{H}} + \sigma^2\boldsymbol{I})^{-1}\boldsymbol{D}\boldsymbol{f}_i \\ &\overset{(a)}{=} v - J^{-1}\sum_{k=0}^{J-1}\frac{|v|^2|D(k,k)|^2}{v|D(k,k)|^2 + \sigma^2} \triangleq \omega\end{aligned} \tag{12}$$

where $\boldsymbol{f}_i$ is the ith column of $\boldsymbol{F}$, and step (a) follows by utilizing (4) and the fact that $\boldsymbol{D}$ is diagonal. Now substitute (12) into (9a). With some straightforward manipulations, we arrive at (11). ■

Lemma 2: The ESE output z_i^{EXT} can be expressed as

$$z_i^{\mathrm{EXT}} = x_i + n_i^{\mathrm{EXT}}\,, \tag{13a}$$

where n_i^{EXT} is independent of x_i, and

$$\mathrm{E}[n_i^{\mathrm{EXT}}] = 0 \ \text{and}\ \mathrm{E}[|n_i^{\mathrm{EXT}}|^2] = 1/\rho^{\mathrm{EXT}}\,. \tag{13b}$$

Proof: Substituting (8c) and (6a) into (8a), we obtain

$$\begin{aligned}\hat{z}_i &= z_i + v\boldsymbol{f}_i^{\mathrm{H}}\boldsymbol{D}^{\mathrm{H}}(v\boldsymbol{D}\boldsymbol{D}^{\mathrm{H}} + \sigma^2\boldsymbol{I})^{-1}\boldsymbol{F}(\boldsymbol{y} - \boldsymbol{Hz}) \\ &= v\boldsymbol{f}_i^{\mathrm{H}}\boldsymbol{D}^{\mathrm{H}}(v\boldsymbol{D}\boldsymbol{D}^{\mathrm{H}} + \sigma^2\boldsymbol{I})^{-1}\boldsymbol{F}(\boldsymbol{y} - \boldsymbol{H}\boldsymbol{z}_{\sim i}) \\ &\quad + \left(1 - v\boldsymbol{f}_i^{\mathrm{H}}\boldsymbol{D}^{\mathrm{H}}(v\boldsymbol{D}\boldsymbol{D}^{\mathrm{H}} + \sigma^2\boldsymbol{I})^{-1}\boldsymbol{D}\boldsymbol{f}_i\right)z_i \\ &= v\boldsymbol{f}_i^{\mathrm{H}}\boldsymbol{D}^{\mathrm{H}}(v\boldsymbol{D}\boldsymbol{D}^{\mathrm{H}} + \sigma^2\boldsymbol{I})^{-1}\boldsymbol{F}(\boldsymbol{y} - \boldsymbol{H}\boldsymbol{z}_{\sim i}) + v^{-1}\omega z_i\end{aligned} \tag{14}$$

where $\boldsymbol{z}_{\sim i}$ represents the vector obtained by setting the ith entry of $\boldsymbol{z}$ to zero, and the last equality follows from (12). Then

$$\begin{aligned}z_i^{\mathrm{EXT}} &\overset{(a)}{=} \frac{v}{\omega\rho^{\mathrm{EXT}}}\cdot\boldsymbol{f}_i^{\mathrm{H}}\boldsymbol{D}^{\mathrm{H}}(v\boldsymbol{D}\boldsymbol{D}^{\mathrm{H}} + \sigma^2\boldsymbol{I})^{-1}\boldsymbol{F}(\boldsymbol{y} - \boldsymbol{H}\boldsymbol{z}_{\sim i}) \\ &\overset{(b)}{=} \frac{v}{\omega\rho^{\mathrm{EXT}}}\cdot\boldsymbol{f}_i^{\mathrm{H}}\boldsymbol{D}^{\mathrm{H}}(v\boldsymbol{D}\boldsymbol{D}^{\mathrm{H}} + \sigma^2\boldsymbol{I})^{-1}\boldsymbol{D}\boldsymbol{f}_i x_i + n_i^{\mathrm{EXT}} \\ &\overset{(c)}{=} x_i + n_i^{\mathrm{EXT}}\end{aligned} \tag{15}$$

where step (a) follows by substituting (14) into (9b) and by

noting $v_i^{\mathrm{EXT}} = 1/\rho^{\mathrm{EXT}}$ and $\omega = \Omega(i, i)$, (*b*) by substituting (6b) and letting

$$n_i^{\mathrm{EXT}} = \frac{v}{\omega\rho^{\mathrm{EXT}}} \cdot \boldsymbol{f}_i^{\mathrm{H}} \boldsymbol{D}(v\boldsymbol{D}^{\mathrm{H}}\boldsymbol{D} + \sigma^2\boldsymbol{I})^{-1}\boldsymbol{F}(\boldsymbol{H}(\boldsymbol{x}_{\sim i} - \boldsymbol{z}_{\sim i}) + \boldsymbol{\eta}), \quad (16)$$

and (*c*) from (12) and (9a). Clearly, n_i^{EXT} in (16) is independent of x_i. Finally, based on (16), (13b) can be readily verified. ■

Intuitively, with sufficient independent components in (16), n_i^{EXT} is Gaussian distributed by invoking the central limit theorem. This idea is made concrete in the lemma below. The details are omitted here due to space limitation.

Lemma 3: If the diagonal entries of $\boldsymbol{D}$ in (6a) are independent and identically distributed (*iid*), then n_i^{EXT} in (13a) converges in distribution to $\mathcal{CN}(0, 1/\rho^{\mathrm{EXT}})$ as $J \to \infty$.

It is required in Lemma 3 that the diagonal entries of $\boldsymbol{D}$ are *iid*. This can be met using the following convention. Denote by $\boldsymbol{D}'$ an arbitrary diagonal channel. Suppose that the transmitted signal is permuted by a random permutation $\boldsymbol{T}$. Then, the equivalent channel becomes $\boldsymbol{D} = \boldsymbol{T}\boldsymbol{D}'\boldsymbol{T}^{\mathrm{H}}$. As a result, the diagonal elements of $\boldsymbol{D}$ are *iid* as $J \to \infty$.

Lemmas 1-3 reveals that the ESE output can be approximated as observations from an AWGN channel with SNR = ρ^{EXT}. Based on this result, we next establish an area theorem for the LP-ILMMSE scheme.

IV. Performance Analysis of LP-ILMMSE Schemes

A. Fundamental Assumptions

In iterative detection, the ESE and DEC are executed in an alternating fashion. The term *one iteration* means that the ESE and DEC are executed in turn each only once. We use a parenthesized superscript to distinguish the variables related to different iterations. For example, we use $\alpha^{(l)}$ to represent the ESE input at the *l*th iteration (and it also represents the DEC output in the (l−1)st iteration). Note that such superscripts may be dropped in situations without causing ambiguity.

For each $\alpha^{(l)}$, assume that there exists a set of random variables $\{A_0^{(l)}, A_1^{(l)}, ..., A_{J-1}^{(l)}\}$ such that

a) each $\alpha_i^{(l)}$ is related to $A_i^{(l)}$ as $\alpha_i^{(l)}(k) = p(x_i = s_k \mid A_i^{(l)})$;

b) $A_i^{(l)}$ is independent of $A_n^{(l)}$ for any $i \neq n$;

c) the probability rule governing the generation of $A_i^{(l)}$ is invariant with respect to the index i, i.e.,

$$p(x_i = s_k \mid A_i^{(l)} = a) = p(x_n = s_k \mid A_n^{(l)} = a).$$

Similar assumptions apply to the DEC input β. We can see from (10) that the corresponding random variable related to each β_i is z_i^{EXT}. We further assume that

d) A_i and z_i^{EXT} are conditionally independent given each x_i.

Assumptions a)-c) are asymptotically true as the block length J tends to infinity if a random-structured code (such as a low-density parity-check (LDPC) code or a conventional FEC code with random interleaving) is used. Assumption d) can be met by following the turbo principle in generating the ESE and DEC outputs. These assumptions are commonly used in analyzing iterative detection algorithms [2][4][5][8].

B. MSE Measure

Define the output mean-square error (MSE) for the ESE at the *l*th iteration as

$$MSE_{\mathrm{ESE}}^{(l)} = \mathrm{E}\left[\left|x_i - \mathrm{E}[x_i \mid A_i^{(l)}, z_i^{\mathrm{EXT}(l)}]\right|^2\right]. \quad (17a)$$

Note that the above MSE is invariant with respect to the index i due to assumption c). Based on Lemma 3, we denote the MSE in (17a) as a function of the output SNR of the ESE as

$$MSE_{\mathrm{ESE}}^{(l)} = \Phi(\rho^{\mathrm{EXT}(l)}). \quad (17b)$$

Similarly, define the output MSE at the *l*th iteration as

$$MSE_{\mathrm{DEC}}^{(l)} = \mathrm{E}\left[\left|x_i - \mathrm{E}[x_i \mid z_i^{\mathrm{EXT}(l)}, A_i^{(l+1)}]\right|^2\right]. \quad (18a)$$

Similarly to (17b), we denote

$$MSE_{\mathrm{DEC}}^{(l)} = \Psi(\rho^{\mathrm{EXT}(l)}). \quad (18b)$$

The MSEs defined in (17) and (18) form a monotonically decreasing sequence as

$$MSE_{\mathrm{ESE}}^{(1)} \geq MSE_{\mathrm{DEC}}^{(1)} \geq MSE_{\mathrm{ESE}}^{(2)} \geq ... \geq MSE_{\mathrm{ESE}}^{(l)} \geq MSE_{\mathrm{DEC}}^{(l)} \geq ... \quad (19)$$

An interpretation of (19) is that the qualities of both the ESE and DEC output improve with iteration. Due to the non-negativity of MSE, the sequence in (19) eventually converges to $MSE^{(\infty)} \geq 0$. We say that the iterative receiver performs *error-free decoding* and the corresponding rate is *achievable* if $MSE^{(\infty)} = 0$.

C. Curve-Matching Property

The monotonic MSE sequence in (19) yields

$$\Phi(\rho^{(l)}) = MSE_{\mathrm{ESE}}^{(l)} \geq MSE_{\mathrm{DEC}}^{(l)} = \Psi(\rho^{(l)}), \text{ for every } l. \quad (20)$$

From the continuity of Φ and Ψ, we can express the above condition alternatively as

$$\Phi(\rho) \geq \Psi(\rho), \text{ for } \rho \in [\rho^{(1)}, \rho^{(\infty)}). \quad (21)$$

The definition in (17) implies that the Φ-function is defined only in $[\rho^{(1)}, \rho^{(\infty)})$. We next extend the definition of Φ to the entire range of $[0, \infty)$. Define the γ-function as

$$\gamma(\rho) = \mathrm{E}\left[\left|x - \mathrm{E}[x \mid z]\right|^2\right] \quad (22)$$

where $z = x + n$, x is uniform over $\mathcal{S}$, and n is independently drawn from $\mathcal{CN}(0, 1/\rho)$. Comparing (18) and (22), we obtain

$$\gamma(\rho) \geq \Psi(\rho), \text{ for any } \rho \in [0, \infty). \quad (23)$$

We now extend the Φ-function as follows:

$$\Phi(\rho) = \gamma(\rho), \text{ for } \rho \in [0, \rho^{(1)}); \text{ and} \quad (24a)$$

$$\Phi(\rho) = 0, \text{ for } \rho \in [\rho^{(\infty)}, \infty). \quad (24b)$$

Together with (21) and (23), we have

$$\Phi(\rho) \geq \Psi(\rho), \text{ for } \rho \in [0, \infty). \quad (25)$$

We are particularly interested in the situation that the ESE and DEC are *matched*, i.e.

$$\Phi(\rho) = \Psi(\rho), \text{ for } \rho \in [0, \infty). \quad (26)$$

D. Area Theorem

Now we are ready to present the main result of this paper.

Theorem 1: If the DEC follows the *a posteriori* probability (APP) decoding principle, then an upper bound of the achievable rate R of the LP-ILMMSE scheme is given by

$$R \leq \int_0^{\infty} \Phi(\rho)\mathrm{d}\rho. \quad (27)$$

The equality holds when the ESE and DEC are matched.

Proof: From Lemmas 1-3, the DEC input is a sequence from an AWGN channel with SNR = ρ^{EXT}. If the DEC performs the optimal APP decoding, then the MSE in (18a) becomes the output MMSE of the DEC. Thus, using [5, Lemma 1], we obtain

$$R = \int_0^{\infty} \Psi(\rho)\mathrm{d}\rho\,.$$

Together with (25) and (26), we arrive at (27). ■

To evaluate the rate using (27), we need the MSE defined in (17a), which requires the probability model of the ESE input $\{\alpha_i\}$ (or equivalently, $\{A_i\}$). Given the FEC code and the decoding operation, $\{\alpha_i\}$ can be generated by simulating the DEC over an AWGN channel (as pointed out in Lemmas 1-3). However, this method is not convenient in system design (which may involve a huge pool of candidate FEC codes). An alternative approach is to assume a probability model in the generation of $\{\alpha_i\}$. It is observed that, for BPSK or QPSK modulation, the DEC output $\{A_i\}$ can be approximated as observations from an AWGN channel [4][10]. Later, we will show by numerical results that this AWGN approximation is also reasonably good for superposition coded modulation (SCM) [14] (though it may be not so good for other higher order modulation methods).

V. Optimization of Power Allocation Matrix

Now, based on the above area theorem, we consider the optimization of the power allocation matrix $\boldsymbol{W}$ to maximize the achievable rate of the proposed scheme. Note that the choice of $\boldsymbol{W}$ affects the equivalent channel in (6) and hence the Φ-function (that characterizes the behavior of the ESE). Thus, we formulate:

$$\text{maximize} \qquad R = \int_0^{+\infty} \Phi(\rho)\mathrm{d}\rho \tag{28a}$$

$$\text{subject to} \qquad \sum_{i=0}^{J-1} \left|W(i,i)\right|^2 \le P\,. \tag{28b}$$

In the above, P is the maximum input power of the channel (1).

It can be verified that, for Gaussian signaling, the solution to (28) is the well-known water-filling power allocation [11]. However, for discrete signaling, water-filling is not necessarily optimal. The optimal solution to (28) with constrained signaling is generally difficult to find. We next show that (28) can be efficiently solved by imposing an AWGN assumption on the ESE input.

Lemma 4: If the ESE inputs $\{A_i\}$ are independent observations from an AWGN channel, then the upper bound in (27) can be expressed as

$$R \le \log|\mathcal{S}| - \int_0^{+\infty} \gamma(\rho + \phi(\gamma(\rho)))\mathrm{d}\rho \tag{29}$$

where the ϕ-function represents the function of ρ^{EXT} against v in (11), and the γ-function is defined in (22).

Proof: Let ρ be the ESE input SNR, and ρ^{EXT} be the ESE output SNR. Then, the ESE input variance is $v = \gamma(\rho)$, and

$$\rho^{\mathrm{EXT}} = \phi(\gamma(\rho)) \equiv \tau(\rho)\,.$$

With Lemma 3 and the AWGN assumption on the ESE inputs, A_i and z_i^{EXT} are (conditionally independent) observations of x_i from AWGN channels. Thus, A_i and z_i^{EXT} can be combined to be a single observation of x_i from an AWGN channel with SNR $= \rho^{\mathrm{TL}}$ (cf., (9a) in [8]), where

$$\rho^{\mathrm{TL}} = \rho^{\mathrm{EXT}} + \rho = \rho^{\mathrm{EXT}} + \tau^{-1}(\rho^{\mathrm{EXT}}) = \rho + \tau(\rho)\,. \tag{30}$$

Thus, we can express the MSE in (17) as

$$MSE_{\mathrm{ESE}} = \Phi(\rho^{\mathrm{EXT}}) = \gamma(\rho^{\mathrm{TL}}) \qquad \text{for } 0 \le \rho \le \infty \tag{31a}$$

$$= \gamma(\rho + \tau(\rho)) \qquad \text{for } 0 \le \rho \le \infty \tag{31b}$$

$$= \gamma(\rho^{\mathrm{EXT}} + \tau^{-1}(\rho^{\mathrm{EXT}})) \qquad \text{for } \tau(0) \le \rho^{\mathrm{EXT}} \le \tau(\infty). \tag{31c}$$

Then, $R \overset{(a)}{\le} \int_0^{\tau(0)} \gamma(\rho)\mathrm{d}\rho + \int_{\tau(0)}^{\tau(\infty)} \gamma(\rho^{\mathrm{EXT}} + \tau^{-1}(\rho^{\mathrm{EXT}}))\mathrm{d}\rho^{\mathrm{EXT}}$

$$\overset{(b)}{=} \int_0^{\tau(0)} \gamma(\rho)\mathrm{d}\rho + \int_{\tau(0)}^{\infty} \gamma(\rho^{\mathrm{TL}})\mathrm{d}\rho^{\mathrm{TL}} - \int_0^{\infty} \gamma(\rho + \tau(\rho))\mathrm{d}\rho$$

$$\overset{(c)}{=} \log|\mathcal{S}| - \int_0^{\infty} \gamma(\rho + \phi(\gamma(\rho)))\mathrm{d}\rho$$

where step (*a*) follows from (27), (24), and (31c), (*b*) from (30) and (31), and (*c*) from $\int_0^{\infty} \gamma(\rho)\mathrm{d}\rho = \log|\mathcal{S}|$ (cf., [7]). ■

Lemma 5: The upper bound in (29) is a concave function of $\{|W(i,i)|^2\}$, provided that $\gamma(\rho)$ is a convex function of ρ.

Proof: It can be shown that the harmonic mean

$$f(z_0, \ldots, z_{J-1}) = \left(J^{-1}\sum_{i=0}^{J-1} 1/z_i\right)^{-1}$$

is concave in $\{z_i\}_{i=0}^{J-1}$ for $z_i > 0$, $0 \le i \le J-1$. Let

$$z_i = 1/\gamma(\rho) + |\Delta(i,i)|^2 |W(i,i)|^2 / \sigma^2\,.$$

Thus, ϕ in (11) is concave in $\{|W(i,i)|^2\}$. Together with the fact that γ is convex and non-increasing (c.f., [12] for the monotony of γ in ρ), $\gamma(\rho + \phi(\gamma(\rho)))$ is convex in $\{|W(i,i)|^2\}$ according to the composition rule of convex functions (cf., Chapter 3.2.4, [13]). Nonnegative weighted sums preserve convexity. Thus

$$\int_0^{+\infty} \gamma(\phi(\gamma(\rho)) + \rho)\mathrm{d}\rho$$

is convex in $\{|W(i,i)|^2\}$, which concludes the proof. ■

The γ-function is convex for most commonly used signaling constellations [12]. Then, from Lemmas 4 and 5, the problem in (28) can be solved using convex programming [13].

VI. Numerical Results

We now provide numerical examples to demonstrate the achievable performance of the LP-ILMMSE scheme. Consider a randomly generated 2×2 MIMO 3-tap ISI channel with the tap coefficients given by

$$\begin{bmatrix} 0.5339 + \mathrm{j}0.5395 & -0.4245 + \mathrm{j}0.0648 \\ -0.3347 - \mathrm{j}0.3727 & -0.4672 - \mathrm{j}0.2420 \end{bmatrix}, \tag{32a}$$

$$\begin{bmatrix} 0.0582 - \mathrm{j}0.2706 & 0.1525 - \mathrm{j}0.7565 \\ -0.4968 - \mathrm{j}0.1543 & -0.5243 - \mathrm{j}0.5915 \end{bmatrix}, \tag{32b}$$

and

$$\begin{bmatrix} -0.5262 - \mathrm{j}0.2654 & -0.3714 - \mathrm{j}0.2865 \\ 0.6721 - \mathrm{j}0.1635 & 0.1607 - \mathrm{j}0.2695 \end{bmatrix}. \tag{32c}$$

The block length $J = 256$. The AWGN assumption is imposed on the ESE input, so that the optimal precoder can be obtained by solving (28) using convex optimization. SCM constellations are used for signaling, with each SCM layer QPSK modulated. The power levels for the 2-layer SCM constellation are $\{p_1 = 0.79, p_2 = 0.21\}$, and those for the 3-layer case are $\{p_1 = 0.61, p_2 = 0.295, p_3 = 0.095\}$. These coefficients are obtained by a brute-force search for maximizing the achievable rate at channel SNR = 10 dB.

Fig.2 illustrates the maximum achievable rate of the above LP-ILMMSE scheme. The water-filling capacity of the channel is also included for comparison. We see from Fig.2 that, at a relatively low rate, the one-layer scheme performs close to the water-filling capacity. As the rate increases, more layers are required to maintain near-capacity performance.

We next verify that the performance limit in Fig.2 is indeed approachable. Consider the above 3-layer SCM scheme. Each SCM layer employs an individual irregular LDPC code with QPSK modulation. We basically follow the approach proposed in [15] in the design of curve-matching irregular LDPC codes. The variable and parity-check edge degree distribution pairs of the optimized LDPC codes are given by $\{\lambda_1(x) = 0.2551x + 0.1529x^2 + 0.0667x^4 + 0.1286x^5 + 0.1520x^{12} + 0.0385x^{13} + 0.0010x^{35} + 0.2052x^{36}, \mu_1(x) = x^7\}$, $\{\lambda_2(x) = 0.2754x + 0.1738x^2 + 0.1140x^5 + 0.0444x^6 + 0.0131x^{10} + 0.0752x^{12} + 0.0908x^{13} + 0.0109x^{35} + 0.2023x^{36}, \mu_2(x) = x^8\}$, and $\{\lambda_3(x) = 0.3712x + 0.2110x^2 + 0.0797x^9 + 0.1916x^{10} + 0.0495x^{26} + 0.0971x^{27}, \mu_3(x) = x^6\}$. The system throughput is 6 bits per channel use.

Fig.3 shows the simulated BER performance of the above LP-ILMMSE scheme with superimposed LDPC codes. The water- filling capacity and the performance limits of the LP-ILMMSE scheme with 2-layer/3-layer SCM are also included for comparison. The 0.6 dB gap between the water-filling capacity and the 3-layer SCM is due to the constrained signaling of the latter. The 0.5 dB gap between 3-layer SCM and the design threshold results mainly from the slight mismatch of the ESE and DEC transfer curves (due to the sub-optimality of the design method in [15]). At code length $\approx 10^5$, the required SNR of the proposed scheme at BER = 10^{-5} is about 11.4 dB, which is only 0.2 dB away from the design threshold.

VII. Conclusions

We show that the ESE output of the proposed LP-ILMMSE scheme can be approximately modeled as a sequence of observations from an AWGN channel. Based on this result, we establish an area theorem to evaluate the achievable rate of the LP-ILMMSE scheme. We also discuss the design of the optimal precoder to maximize the achievable rate of the scheme. Numerical results show that the analytical performance limit is approachable using superimposed LDPC codes for FEC coding.

Acknowledgements

This work has been performed in the framework of the ICT project ICT-248894 WHERE2, funded by the European Union.

References

[1] C. Berrou, A. Glavieux, and P. Thitimajshima, "Near Shannon limit error-correcting coding and decoding: turbo-codes," in *Proc. ICC'93,* Geneve, Switzerland, May 1993.

[2] T. Richardson, A. Shokrollahi and R. Urbanke, "Design of capacity-approaching irregular low-density parity-check codes," *IEEE Trans. Inform. Theory*, vol. 47, no. 2, pp. 619-637, Feb. 2001.

[3] A. Ashikhmin, G. Kramer, and S. ten Brink, "Extrinsic information transfer functions: Model and erasure channel properties," *IEEE Trans. Inf. Theory*, vol. 50, no. 11, pp. 2657–2673, Nov. 2004.

[4] S. ten Brink, "Convergence behavior of iteratively decoded parallel concatenated codes," *IEEE Trans. Commun.*, vol. 49, no. 10, pp. 1727–1737, Oct. 2001.

[5] K. Bhattad and K. R. Narayanan, "An MSE-based transfer chart for analyzing iterative decoding schemes using a Gaussian approximation," *IEEE trans. Inform. Theory*, vol. 53, no. 1, Jan. 2007.

[6] X. Yuan, C. Xu, Li Ping, and X. Lin, "Precoder design for MIMO ISI multiple-access channels based on iterative LMMSE detection," *IEEE J. Select. Topics in Signal Processing*, vol. 3, no. 6, pp. 1118-1128, 2009.

[7] D. Guo, S. Shamai, and S. Verdú, "Mutual information and minimum mean-square error in Gaussian channels," *IEEE Trans. Inform. Theory*, vol. 51, no. 4, April 2005.

[8] X. Yuan and Li Ping, "Achievable rates of coded linear systems with iterative MMSE detection," in *Proc. IEEE Globecom'09*, Honolulu, HI, USA, Nov. 30 – Dec. 4 2009.

[9] S. M. Kay, *Fundamentals of Statistical Signal Processing: Estimation Theory*, Upper Saddle River, NJ: Prentice Hall PTR, 1993.

[10] S. Y. Chung, T. J. Richardson, and R. L. Urbanke, "Analysis of sum-product decoding of low-density parity-check codes using a Gaussian approximation," *IEEE Trans. Inf. Theory*, vol. 47, no. 2, pp. 657-670, Feb. 2001.

[11] T. M. Cover, and J. A. Thomas, *Elements of Information Theory*, Wiley, New York, 1991.

[12] D. Guo, Y. Wu, S. Shamai, S. Verdú, "Estimation in Gaussian noise: Properties of the minimum mean-square error," *Preprint*.

[13] S. Boyd and L. Vandenberghe, *Convex Optimization*, Cambridge: Cambridge University Press, 2004.

[14] U. Wachsmann, R. F. H. Fischer, and J. B. Huber, "Multilevel codes: theoretical concepts and practical design rules," *IEEE Trans. Inform. Theory*, vol. 45, no. 5, pp. 1361–1391, July 1999.

[15] K. R. Narayanan, D. N. Doan, and R. V. Tamma, "Design and analysis of LDPC codes for turbo equalization with optimal and suboptimal soft output equalizers," in *Proc. Allerton Conf. Communications, Control, and Computing*, Monticello, IL, Oct. 2002, pp. 737–746.

[16] M. Payaró and D. P. Palomar, "On optimal precoding in linear vector Gaussian channels with arbitrary input distribution," in *Proc. IEEE International Symposium on Information Theory (ISIT'09)*, Seoul, Korea, Jun. 2009.

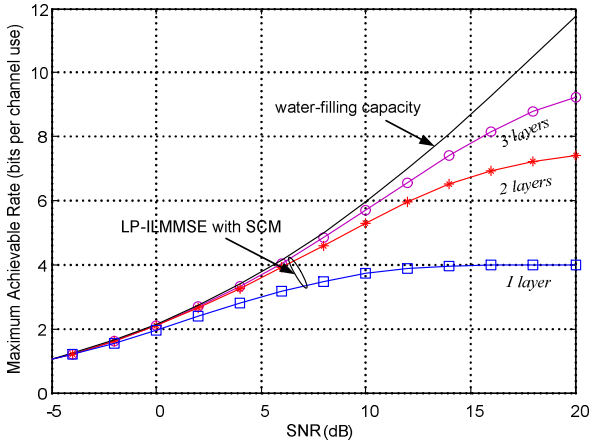

Fig. 2. The maximum achievable rates of LP-ILMMSE with SCM in the MIMO ISI channel (32). The power levels for the 2-layer case are $\{p_1 = 0.79, p_2 = 0.21\}$, and those for the 3-layer case are $\{p_1 = 0.61, p_2 = 0.295, p_3 = 0.095\}$.

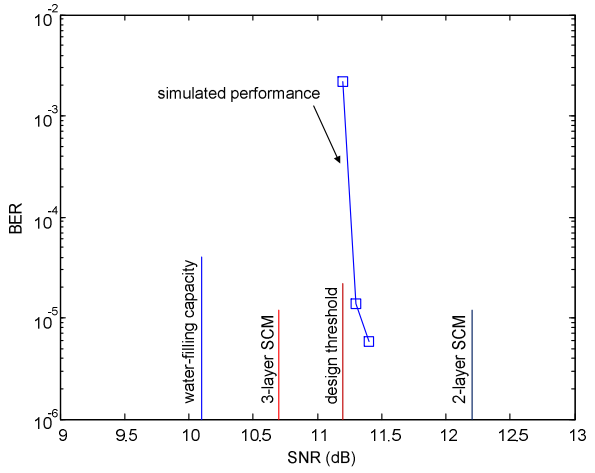

Fig. 3. The BER performance of the proposed LP-ILMMSE scheme with SCM over the MIMO ISI channel (32). Each SCM layer k employs an irregular LDPC code with the degree distribution pair given by $\lambda_k(x)$ and $\mu_k(x)$.